Tullius, T. D., Frank, P., & Hodgson, K. O. (1978) *Proc. Natl. Acad. Sci. U.S.A. 75*, 4069-4073.
Ugurbil, K., & Bersohn, R. (1977) *Biochemistry 16*, 3016-3023.
Ugurbil, K., Norton, R. S., Allerhand, A., & Bersohn, R. (1977) *Biochemistry 16*, 886-894.
Vänngård, T. (1972) in *Biological Applications in Electron Spin Resonance* (Swartz, H. M., Bolton, J. R., & Borg, D. C., Eds.) pp 411-447, Wiley-Interscience, New York.
Vin Rijn, J., Driessen, W. L., Reedijk, J., & Lehn, J.-M. (1984) *Inorg. Chem. 23*, 3584-3588.
Wherland, S., & Pecht, I. (1978) *Biochemistry 17*, 2585-2591.
Woodruff, W. H., Norton, K. A., Swanson, B. I., & Fry, H. A. (1984) *Proc. Natl. Acad. Sci. U.S.A. 81*, 1263-1267.
Yokoi, H., & Addison, A. W. (1977) *Inorg. Chem. 16*, 1341-1349.

Picosecond Resolution of Tyrosine Fluorescence and Anisotropy Decays by 2-GHz Frequency-Domain Fluorometry†

Joseph R. Lakowicz,* Gabor Laczko, and Ignacy Gryczynski
Department of Biological Chemistry, University of Maryland School of Medicine, Baltimore, Maryland 21201
Received May 1, 1986; Revised Manuscript Received September 11, 1986

ABSTRACT: We extended the technique of frequency-domain fluorometry to an upper frequency limit of 2000 MHz. This was accomplished by using the harmonic content of a laser pulse train (3.76 MHz, 5 ps) from a synchronously pumped and cavity-dumped dye laser. We used a microchannel plate photomultiplier as the detector to obtain the 2-GHz bandwidth. This new instrument was used to examine tyrosine intensity and anisotropy decays from peptides and proteins. These initial data sets demonstrate that triply exponential tyrosine intensity decays are easily recoverable, even if the mean decay time is less than 1 ns. Importantly, the extended frequency range provides good resolution of rapid and/or multiexponential tyrosine anisotropy decays. Correlation times as short as 15 ps have been recovered for indole, with an uncertainty of ±3 ps. We recovered a doubly exponential anisotropy decay of oxytoxin (29 and 454 ps), which probably reflects torsional motions of the phenol ring and overall rotational diffusion, respectively. Also, a 40-ps component was found in the anisotropy decay of bovine pancreatic trypsin inhibitor, which may be due to rapid torsional motions of the tyrosine residues and/or energy transfer among these residues. The rapid component has an amplitude of 0.05, which is about 16% of the total anisotropy. The availability of 2-GHz frequency-domain data extends the measurable time scale for fluorescence to overlap with that of molecular dynamics calculations.

There is considerable interest in obtaining picosecond time resolution of the intrinsic fluorescence from proteins. The time-resolved intensity decay parameters may be correlated with structural features of the proteins. The anisotropy decay times may be compared with calculations of segmental motions or with hydrodynamic theories for global rotational diffusion. There are two alternative methods to obtaining the time-dependent data. These are direct measurements in the time domain (O'Connor & Phillips, 1985; Cundall & Dale, 1980; Brand et al., 1985) or measurements in the frequency domain (Lakowicz et al., 1984a,b; Lakowicz, 1985, 1986a,b). The time-domain measurements are dominant because of the availability of instrumentation, the increasing availability of picosecond pulsed laser sources, and the intuitive advantages of seeing the time-resolved data. Surprisingly, these instruments have yielded rather few direct measurements of the decays of protein fluorescence or anisotropy (Lee et al., 1985; Ludescher et al., 1985). We know of no tyrosine anisotropy decays obtained with a picosecond laser source, but intensity decays of tyrosine have been reported for histone H1 (Libertini & Small, 1985), and the intensity decays of a variety of phenol and tyrosine derivatives have been examined by using pulse synchrotron radiation with pulse widths near 500 ps (Laws et al., 1986). Picosecond tryptophan intensity decays have been observed for hemoglobin (Albuni et al., 1985), which illustrates the need for picosecond resolution of protein fluorescence.

Scheme I

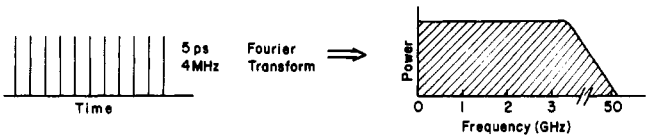

During the past 3 years, this laboratory and others have developed instrumentation for variable-frequency phase-modulation fluorometry (Lakowicz & Maliwal, 1985; Lakowicz et al., 1986a; Gratton & Linkeman, 1983). To date, the upper frequency limit has been about 200 MHz. This limitation was the result of two factors. First, the available light modulators could only provide adequate modulation to about 250 MHz. Second, the time response of standard photomultipliers (1.5-ns full width at half-maximum) limited their bandwidth to about 220 MHz (3dB point; Wilson & Hawkes, 1983). We overcame the 200-MHz limit using two modifications of our original instrument (Lakowicz & Maliwal, 1985). First, we avoided the use of a light modulator by using the intrinsic high-frequency harmonic content of a 5-ps laser

† Dedicated to Professor Gregorio Weber on the occasion of his seventieth birthday. This work was supported by Grant DAAG29-85-G-0017 from the Army Research Office, Grants PCM-8210878 and DMB-08502835 from the National Science Foundation, and Grant GM-29318 from the National Institutes of Health.
* Address correspondence to this author.

0006-2960/87/0426-0082$01.50/0

pulse train. This idea was suggested by Gratton and Lopez-Delgado (1980) for synchrotron radiation (Gratton et al., 1984). The use of a pulse train as a modulated source is illustrated in Scheme I. Our laser produces 5-ps pulses at a repetition rate of 4 MHz. In the frequency domain, this source contains harmonic content at each integer multiple of 4 MHz, up to about 50 GHz. Second, we replaced the photomultiplier tube (PMT)[1] with a microchannel plate (MCP) photomultiplier (Hamamatsu R1564). The single photoelectron pulse width of these devices is 10–20-fold less than that of a standard PMT (Yamazaki et al., 1985), and hence, we expected its bandwidth to extend to 2 GHz. This instrument is the subject of a separate publication (Lakowicz et al., 1986b).

In this paper, we describe our initial observations on tyrosyl peptides and proteins using the 2-GHz instrument. By the recovery of single-exponential decays, we demonstrate the absence of significant systematic errors in the data. For more complex samples, the data demonstrate that multiexponential intensity and anisotropy decays on the picosecond time scale are easily recoverable. Correlation times as short as 15 ps have been measured for indole in nonviscous solvent.

Materials and Methods

Frequency-domain phase and modulation data were measured by using the instrument described previously (Lakowicz & Maliwal, 1985; Lakowicz et al., 1986b), which was modified in several ways. The light source was the 3.7931-MHz cavity-dumped output from a Coherent Model 700 dye laser. The dye was rhodamine 6G. The second jet was used with the saturable absorber DODCI. The dye laser was synchronously pumped by using a mode-locked argon ion laser, Coherent Innova 15, about 800 mW at 514 nm and 76 MHz. The visible output of the dye laser was typically near 60 mW. To obtain UV power for the excitation of tyrosine and indole, we used a Spectra Physics Model 390 frequency doubler, with a KDP angle-tuned crystal. The average UV power was near 0.5 mW, which was attenuated 50–100-fold prior to the sample. For our application, the pulse width and pulse shape are not critical, but the pulse width of the visible output of the dye laser was 5 ps or less.

The frequency synthesizer for cross-correlation detection was phaselocked to the cavity dumper. Our synthesizers have an upper frequency limit of 500 MHz. To obtain frquencies to 2 GHz, we doubled and quadrupled the output. Additionally, it was necessary to cross-correlate the MCP PMT (Hammamatsu R1564) signal after its exit from the PMT housing. This required external mixing, amplification, filtering, and RF shielding. These circuits are described elsewhere in detail (Lakowicz et al., 1986b). Functionally, this system (pulsed source, MCP-PMT, and amplifiers) provides modulation at every integer multiple of 3.7931 MHz. From 20 to 400 MHz, the modulation is near 2; at 1 GHz, the modulation is near 0.5, and this value decreases to 0.1 at 2 GHz.

Unless stated otherwise, all samples were in 0.05 M Tris, pH 7.0. Excitation of tyrosine was at 285–287 nm, where the fundamental anisotropy is 0.32. Emission was observed through a 300-nm interference filter, 10-nm band-pass. Excitation of indole was at 298 nm, where its fundamental anisotropy is 0.29. Indole emission was observed through a band-pass filter (Schott WG-320). Examination of buffer alone indicated background fluorescence and/or scatter was typically 0,5%, and in no case did the background exceed 1%. NAcTyrA (lot 070627), tyrosine (lot 061337), and indole (lot 050747) were from Aldrich. Oxytocin (lot 15F-00021) and synthetic leucine-enkephalin (lot 51F-5816) were from Sigma. BPTI was a gift from K. Wurthrich (Switzerland). Rose bengal was purified by silica thin-layer chromatography using ethanol/ethyl acetate/chloroform (65/25/10).

Theory and Data Analysis

Analysis of the frequency-domain data was described previously in detail for both intensity and anisotropy decays (Lakowicz et al., 1984a,b, 1985; Maliwal & Lakowicz, 1986). For completeness, we briefly describe the procedure. For an intensity decay analysis, the measured quantities are the frequency-dependent phase angles (ϕ_ω) and demodulation factors (m_ω, modulation), where ω is the modulation frequency in radians per second. These values are compared with calculated values ($\phi_{c\omega}$ and $m_{c\omega}$) for any assumed parameter values. Suppose the intensity decay is the sum of exponentials

$$I(t) = \sum_i \alpha_i e^{-t/\tau_i} \tag{1}$$

where τ_i are the decay times and α_i are the preexponential factors. Then

$$\phi_{c\omega} = \arctan (N_\omega / D_\omega) \tag{2}$$

$$m_{c\omega} = (N_\omega^2 + D_\omega^2)^{1/2} \tag{3}$$

where

$$N_\omega = \sum_i \frac{\alpha_i \omega \tau_i^2}{1 + \omega^2 \tau_i^2} \tag{4}$$

$$D_\omega = \sum_i \frac{\alpha_i \tau_i}{1 + \omega^2 \tau_i^2} \tag{5}$$

and $\sum \alpha_i \tau_i = 1$. The steady-state contribution of a component to the total emission is given by

$$f_i = \frac{\alpha_i \tau_i}{\sum_i \alpha_i \tau_i} \tag{6}$$

The goodness of fit is characterized by

$$\chi_R^2 = \frac{1}{\nu} \sum_\omega \frac{1}{\sigma_p^2} (\phi_\omega - \phi_{c\omega})^2 + \frac{1}{\nu} \sum_\omega \frac{1}{\sigma_m^2} (m_\omega - m_{\omega c})^2 \tag{7}$$

where ν is the number of degrees of freedom and σ_p and σ_m are the experimental uncertainties in the phase and modulation values, respectively.

Anisotropy decay parameters are obtained from the frequency-dependent values of the phase difference between the perpendicular and parallel components of the emission ($\Delta_\omega = \phi_\perp - \phi_\parallel$) and the modulated anisotropies [$r_\omega = (\Lambda_\omega - 1)/(\Lambda_\omega + 2)$, where $\Lambda_\omega = m_\parallel / m_\perp$ is the ratio of the polarized modulated amplitudes]. Suppose the anisotropy decay is described by a sum of exponentials;

$$r(t) = r_0 \sum_i g_i e^{-t/\theta_i} \tag{8}$$

where r_0 is the anisotropy in the absence of rotational diffusion, θ_i the correlation times, and g_i the associated amplitudes. For reasons described in detail (Lakowicz et al., 1986a), we prefer to input the known value of r_0 into the analysis. Some analyses were performed with r_0 as a floating parameter. The choice

[1] Abbreviations: BPTI, bovine pancreatic trypsin inhibitor; Enk, [Leu^5]enkephalin (Tyr-Gly-Gly-Phe-Leu); MCP, microchannel plate; NAcTyrA, *N*-acetyl-L-tyrosinamide; oxytocin, Cys-Tyr-Ile-Gln-Asn-Cys-Pro-Leu-Gly-NH_2; PMT, photomultiplier tube; Tris, tris(hydroxymethyl)aminomethane.

Table I: Intensity Decays for Phenol, Tyrosine, and Rose Bengal at 20 °C

sample	n	τ_i (ns)	α_i	f_i	χ_R^2
phenol, 5 mM	1	3.16	1.0	1.0	1.09[a]
acetate, pH 6	2	0.27	0.01	0.001	
		3.17	0.99	0.999	1.07
tyrosine, 5 mM	1	3.27	1.0	1.0	0.92
acetate, pH 6	2	0.98	0.01	0.003	
		3.29	0.99	0.997	0.88
tyrosine, pH 2.1	1	2.55	1.0	1.0	44.5
	2	0.80	0.20	0.06	
		2.85	0.80	0.94	1.1
rose bengal in methanol[b]	1	0.50	1.0	1.0	3.89
	2	0.49	0.99	0.98	
		0.94	0.01	0.02	3.94

[a] $\sigma_p = 0.2°$ and $\sigma_m = 0.005$. [b] Excitation, 575 nm; emission filter, Corning 2.61.

of r_0 is not always certain, especially in proteins like BPTI which have more than one tyrosine residue and the possibility of energy transfer. In the case of indole, we varied its value of r_0 to estimate uncertainties in the value of θ.

The intensity decay of the polarized emission is given by

$$I_{\parallel}(t) = (1/3)I(t)[1 + r(t)] \quad (9)$$

$$I_{\perp}(t) = (1/3)I(t)[1 - 2r(t)] \quad (10)$$

where $I(t)$ is the intensity decay law. In the anisotropy analysis, we use the intensity decay parameters obtained from the use of eq 1–7. The calculated values of Δ_ω and Λ_ω are determined by

$$\Delta_{c\omega} = \arctan\left(\frac{D_{\parallel}N_{\perp} - N_{\parallel}D_{\perp}}{N_{\parallel}N_{\perp} + D_{\parallel}D_{\perp}}\right) \quad (11)$$

$$\Lambda_{c\omega} = \left(\frac{N_{\parallel}^2 + D_{\perp}^2}{N_{\perp}^2 + D_{\perp}^2}\right)^{1/2} \quad (12)$$

where

$$N_i = \int_0^{\infty} I_i(t) \sin \omega t \, dt \quad (13)$$

$$D_i = \int_0^{\infty} I_i(t) \cos \omega t \, dt \quad (14)$$

The goodness of fit is judged by an equation analogous to eq 7.

Results

Simple Intensity Decays. The instrumentation used for this report is new, and there were some questions about the presence of systematic errors which could result in the apparent recovery of extra components in the intensity decays. To demonstrate the absence of significant systematic errors, we show data for three substances, each of which was expected to show a single-exponential intensity decay. The intensity decay of phenol was reported to be a single exponential by Gauduchon and Wahl (1978) and by Laws et al. (1986), who found a decay time of 3.74 ns at 5 °C. We too recovered a single-exponential decay, and our shorter value of 3.16 ns is due to the higher temperature of 20 °C. It should be noted that the data for phenol [Figure 1 (●)] are well matched by the single-exponential model (—) and that the goodness of fit parameter is not improved by fitting to a double-exponential decay (Table I). Attempts to fit the data to a double-exponential decay do not result in a significant decrease in χ_R^2, and the amplitude of the second component is less than 1%. In a similar manner, the decay of rose bengal in methanol was

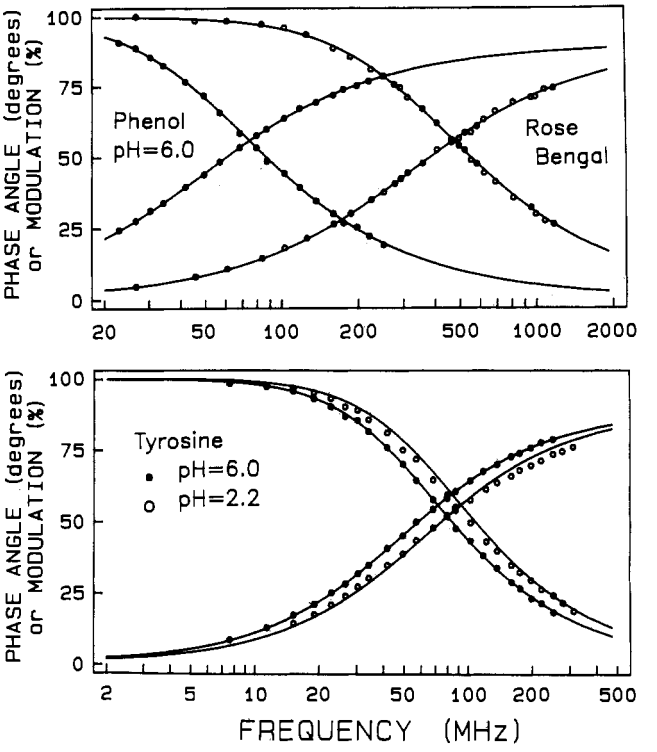

FIGURE 1: Frequency-domain intensity decays for phenol, tyrosine, and rose bengal, 20 °C. In each case, the symbols show the data and the solid lines the best single-exponential fits. (Top) Phenol (●); rose bengal (○). (Bottom) Tyrosine, pH 6.0 (●); tyrosine, pH 2.2 (○). The phase angle increases and the modulation decreases with increasing modulation frequency. See Table I for more details.

also found to be a single exponential (Figure 1 and Table I). Hence, the measurements appear to be free of systematic errors from 10 to 1200 MHz, and in other testing, we did not detect systematic errors to 2000 MHz (Lakowicz et al., 1986b). The measurements for tyrosine itself at pH 6 also indicated a single-exponential decay. These results are in agreement with those of Laws et al. (1986), who also reported only a single-exponential decay. At pH 2, the decay becomes distinctly double exponential, as can be seen from the mismatch of the data (○) to the single-exponential model (Figure 1) and the 40-fold decrease in χ_R^2 for the double-exponential fit. From these four sets of data, and other extensive testing (Lakowicz et al., 1986b), we believe that systematic errors, if present, do not affect the recovered parameters.

Tyrosyl Intensity Decays. Frequency-domain data are shown in Figure 2 for NAcTyrA and Leu-enkephalin. These data were analyzed with various numbers of exponential components, and the results are summarized in Table II. The intensity decay of NAcTyrA was found to be at least doubly exponential. The large value of $\chi_R^2 = 86$ and the lack of fit to the data (●) for the single-exponential model (---) indicate its inadequacy. Under our experimental conditions, the decay is characterized as a double exponential with decay times of 0.111 and 1.66 ns. The shorter lived component contributes about 4% of the total emission. Laws and co-workers (Laws et al., 1986) also found a double-exponential decay for NAcTyrA, which they attributed to the rotomer populations. Their data were at a different temperature (5 °C), but a comparison shows that the decay times they recovered were more closely spaced than our values. However, they found that the shorter component contributes about 7% to the total emission, so the difference may be attributed to the effects of temperature or to the different time resolution of the measurements. The deviation from a single-exponential decay law

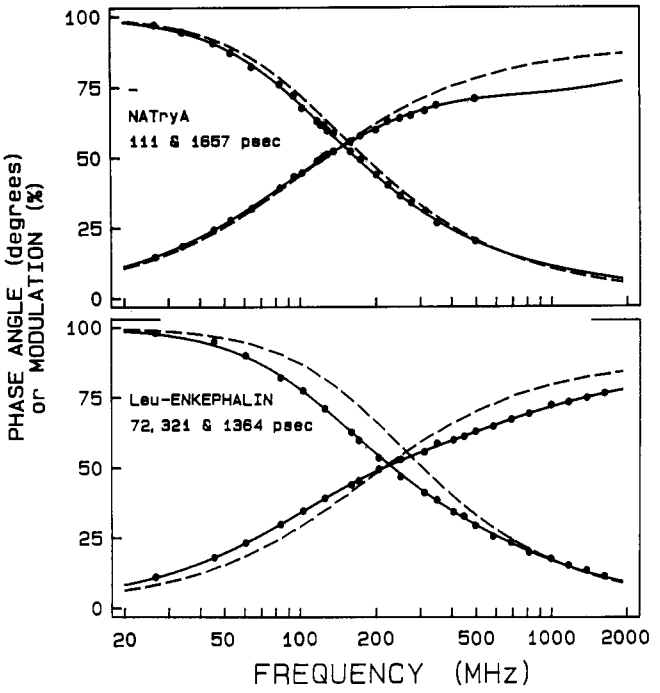

FIGURE 2: Frequency-domain intensity decays of *N*-acetyl-L-tyrosinamide (top) and [Leu^5]enkephalin (bottom) at 20 °C. In each case, the symbols (●) represent the data, the solid line the best three-exponential fit, and the dashed line the best one-exponential fit. The phase angles increase and the modulations decrease with increasing modulation frequency. The decay and goodness of fit parameters are summarized in Table II.

Table II: Intensity Decay Analysis for Tyrosine Emission, 25 °C, pH 7

sample, °C	n^a	τ_i (ps)	$\alpha_i{}^b$	$f_i{}^c$	$\chi_R{}^2$
NAcTyrA, 20	1	1511	1.0	1.0	86[d]
	2	111	0.35	0.04	
		1657	0.65	0.96	2.8
oxytocin, 25	1	634	1.0	1.0	377
	2	140	0.42	0.11	
		833	0.58	0.89	5.9
	3	80	0.29	0.04	
		359	0.28	0.09	
		927	0.43	0.77	2.1
[Leu^5]enkephalin, 20	1	896	1.0	1.0	460
	2	249	0.47	0.14	
		1315	0.53	0.86	3.7
	3	72	0.12	0.01	
		321	0.40	0.17	
		1364	0.48	0.83	1.9
BPTI, 25	1	437	1.0	1.0	543
	2	95	0.50	0.13	
		662	0.50	0.87	3.9
	3	92	0.49	0.12	
		626	0.44	0.73	
		814	0.07	0.16	4.1

[a] Number of exponential components. The underlined value is the fit we considered to be the most appropriate. [b] $\sum\alpha_i = 1.0$. [c] $\sum f_i = 1.0$, $f_i = \alpha_i\tau_i/\sum\alpha_i\tau_i$. [d] Calculated by using 0.2° as the standard deviation of the phase angles and 0.005 as the standard deviation of the modulation.

is greater for the tyrosine emission from Leu-enkephalin. In this case, the single-exponential model (---) provides a very poor match to the data (●) and an extreme value for $\chi_R{}^2$ = 460. Even a double-exponential decay provides a poor fit to the data. The value of $\chi_R{}^2$ decreases 2-fold upon inclusion of a third decay time, which indicates that the third decay time is necessary to account for the data.

Additional frequency-domain data for oxytocin and BPTI are shown in Figure 3. For both molecules, the data are easily

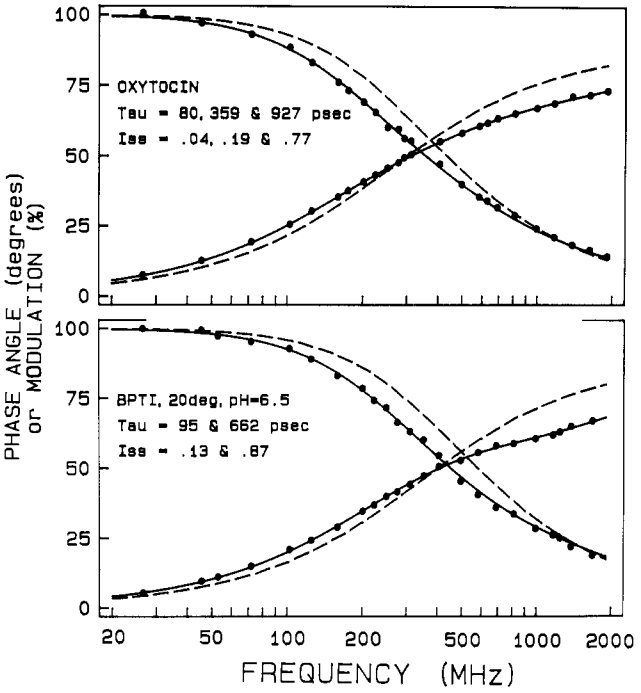

FIGURE 3: Frequency-domain intensity decays of oxytocin (top) and BPTI (bottom) at 25 °C. The symbols (●) represent the data, the dashed line the best one-exponential fit, and the solid line the best three-exponential fit.

adequate to reject the single-exponential model. This is apparent from the lack of overlap of the best single-exponential fits (---) with the experimental data (●). For oxytocin, the data require at least three decay times to obtain an adequate fit, based on the 2.8-fold decrease in $\chi_R{}^2$. For BPTI, two decay times are adequate to explain the data. In this case, the value of $\chi_R{}^2$ did not decrease for the three decay time model (Table II).

Our acceptance of a fit with $\chi_R{}^2$ = 3.9 for BPTI may cause confusion. At present, we do not know the precise values of the uncertainties (σ_p and σ_m) in the phase and modulation values (eq 7). For this reason, the values of $\chi_R{}^2$ are not necessarily near unity for a adequate fit. One reason is that we must estimate the weighting factors used in the least-squares analysis (eq 7). If the estimated values of σ_p and σ_m are too large or too small, then the final values of $\chi_R{}^2$ are too small or too large, respectively. However, this uncertainty does not affect the relative values of $\chi_R{}^2$, and we use the relative values in selecting the appropriate fit. Since BPTI has a low quantum yield, it is not surprising that our usual values of σ_p = 0.2 and σ_m = 0.005 are slightly too small. Additionally, the decay laws are not necessarily a sum of exponentials but may be nonexponential due to a number of factors including the presence of lifetime distributions and/or spectral relaxation.

Simulations of Complex Anisotropy Decays. Prior to examining the experimental data for anisotropy decays, it is informative to identify the effects of segmental mobility and overall rotational diffusion. Simulated data are shown in Figure 4. In this case, the rotational correlation time was assumed to be 4 ns, and the correlation time of the segmental motion was assumed to be 40 ps. The values of Δ_ω and r_ω were calculated by using eq 9–14. If the amplitude of the 40-ps motion is zero, then the differential phase angles are distributed as an approximate Lorentzian (---). If the amplitude of the 40-ps motion accounts for 50% of the anisotropy decay, then a bimodal distribution is seen (—). The short correlation time results in increasing phase angles at the higher frequencies. If the 40-ps motion accounts for all the anisotropy decay, then

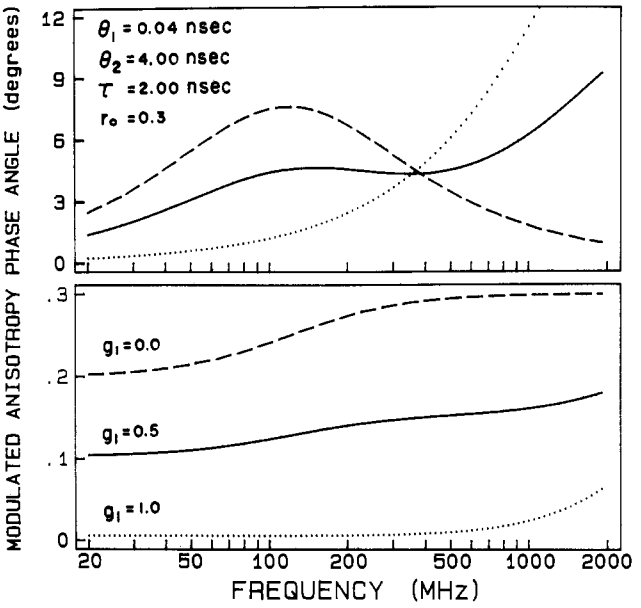

FIGURE 4: Simulated frequency-domain data for rotational diffusion and segmental motions. The simulated data are for a intensity decay time of 2 ns, a rotational correlation time of 4 ns, and a segmental motion of 0.04 ns. The fundamental anisotropy (r_0) is assumed to be 0.30. The fractional amplitude of the 40-ps motion is 0.0 (---), 0.5 (—), and 1.0 (···).

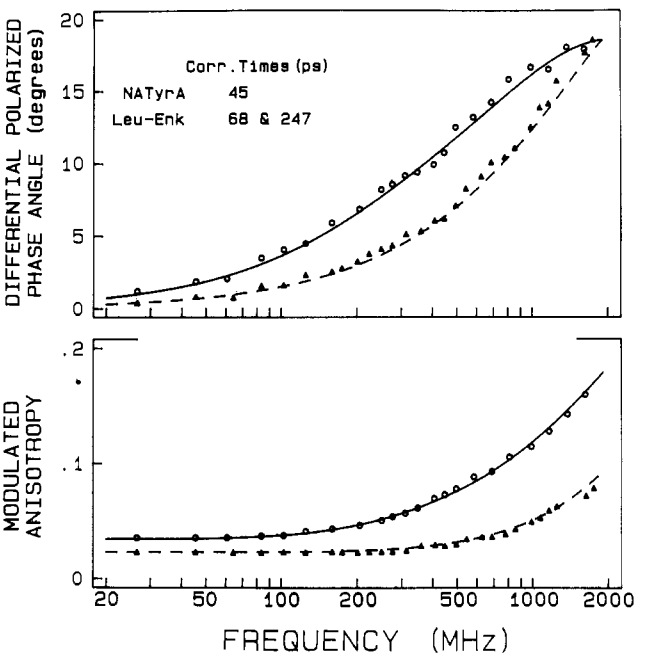

FIGURE 5: Differential phase and modulated anisotropy data for NAcTyrA (▲) and [Leu^5]enkephalin (O) at 20 °C. The NAcTyrA sample also contained 0.5 M KI.

the effect of overall rotational diffusion is eliminated (···).

We also measure the modulated anisotropies (Figure 4, lower panel). These values are analogous to the usual steady-state anisotropies, except that they are calculated by using the polarized and modulated components of the emission (Maliwal & Lakowicz, 1986). The significance of the modulated anisotropy is best illustrated by its values at low and high modulation frequencies. At low frequencies, the value of r_ω is equivalent to the steady-state anisotropy. As the frequency increases, r_ω increases monotonically to r_0, which is the anisotropy in the absence of rotational diffusion. The frequency dependence of r_ω for each anisotropy decay shows an increase near the frequency which is characteristic of the correlation time. Perhaps equally important is the strong dependence of the modulated anisotropy values on the fractional contribution of the rapid motion. We believe that these values minimize the amplitude and range of the correlation times which acceptably explain the phase data. Hence, both phase and modulation data are valuable for determining the anisotropy decay law.

The simulations shown in Figure 4 illustrate the important contribution of the data above 200 MHz. If data were only available to 200 MHz, then the shorter correlation time would be estimated from the flattening of the phase vs. frequency curve in the range from 100 to 200 MHz (—). The data above 200 MHz reflect primarily the shorter correlation time and thereby aid in its determination. However, the simulated data also indicate that still higher frequencies are desirable to reach the Δ_ω maxima of the shorter correlation times.

Experimental Anisotropy Decays. Anisotropy decays of tyrosyl fluorescence were recovered from the frequency-dependent differential phase angles and modulated anisotropies. In a separate publication, we demonstrated that monoexponential anisotropy decays can be recovered, indicating the absence of significant systematic errors in the data (Lakowicz et al., 1986b). Data for NAcTyrA, enkephalin, oxytocin, and BPTI are shown in Figures 5 and 6, and the parameters are summarized (Tables III and IV). NAcTyrA at 20 °C displays a correlation time of 45 ps. This correlation time was

Table III: Tyrosine Anisotropy Decays of Peptides and Proteins from Frequency-Domain Data, pH 7.0[a]

sample	n	θ_i (ps)	$r_0 g_i$	χ_R^2
[Leu^5]enkephalin, 20 °C	1	96	0.320	7.4
	2[f]	68	0.241	
		247	0.08	3.4
	3	67	0.114	
		69	0.127	
		246	0.08	3.5
	2	⟨40⟩[b]	0.126	
		147	0.194	5.2
	2	⟨50⟩	0.164	
		167	0.156	4.3
	2	⟨80⟩	0.260	
		405	0.038	4.5
oxytocin, 25 °C	1	83	0.32	292
	2	29	0.208	
		454	0.112	3.2
	3	28	0.105	
		29	0.104	
		454	0.112	3.4
	2	⟨15⟩[b]	0.177	
		329	0.143	14.2
	2	⟨20⟩	0.189	
		369	0.131	7.7
	2	⟨45⟩	0.240	
		690	0.080	20.9
	2	⟨60⟩	0.262	
		1057	0.058	66.3
BPTI, 25 °C, pH 6.5	1	1559	⟨0.270⟩[c]	3.20
	2	158	0.028[d]	
		2443	0.242	3.6
	2	39	0.049[e]	
		2244	0.250	1.8
	3	24	0.060[e]	
		1211	0.099	
		3618	0.154	1.8
	2	⟨2⟩	0.009[d]	11.2
		1858	0.261	

[a] The three-component intensity decay was used for the correlation time analyses. The total anisotropy was held fixed at r_0 = 0.320 for enkephalin and oxytocin. [b] The broken brackets indicate these values were held fixed at the indicated value. [c] Measured in propylene glycol/water (66/33) at −60 °C. [d] $\sum r_0 g_i$ = 0.27. [e] $\sum r_0 g_i$ is variable in the analysis. [f] The underlined value represents the fit we consider most appropriate for the data.

Table IV: Anisotropy Decays of *N*-Acetyl-L-tyrosinamide in Water[a]

temp (°C)	θ (ps)[b]	r_0[b]	χ_R^2
5	62	⟨0.32⟩	3.0[c]
	59	0.331	2.9
20	45	⟨0.32⟩	4.4
	37	0.37	2.3
58	27	⟨0.32⟩	2.0
	23	0.37	1.7

[a] The solution contained 0.25 M KI to decrease the decay time. The total concentration of KCl + KI was 0.5 M. The buffer was 0.05 M Tris, pH 7.0, containing a trace amount of $Na_2S_2O_3$ to prevent iodine formation. [b] The broken brackets indicate the value of r_0 was fixed in the analysis. The lack of brackets indicates the value of r_0 was a variable parameter in the analysis. The fixed r_0 value was measured at −60 °C for the probe in propylene glycol, using 287-nm excitation. [c] Calculated by using 0.2° and 0.005 as the standard deviations of the phase and modulation, respectively.

easily quantified with nearly 20° of phase shift between the polarized components at 2 GHz. Enkephalin displayed a more complex anisotropy decay, with correlation times of 68 and 247 ps (Figure 5). For enkephalin, about 75% of the anisotropy decays via the faster process, but a longer correlation time is necessary to fit the data (Table III). The data for enkephalin were not adequate to recover three correlation times, if three exist, as indicated by the similarity of the correlation times and the value of χ_R^2 for this more complex model (Table III). It is tempting to assign the 68-ps component to segmental motions of the tyrosyl residue and the 247-ps component to global rotational diffusion of enkephalin. The 247-ps correlation time is close to that expected for enkephalin (Lakowicz & Maliwal, 1983).

We questioned the uncertainty in the 68-ps correlation time found for enkephalin. To accomplish this, we attempted to fit the data using different but fixed values for the shorter correlation time. The other parameter values were allowed to vary to minimize χ_R^2. This procedure thereby takes into account correlation between the parameters. Decreasing θ_1 to 50 ps results in a 1.3-fold increase in χ_R^2. With our 41 degrees of freedom (22 phase angles, 22 polarized ratios, and 3 floating parameters), this 1.3-fold value is adequate to reject the values of 50 and 80 ps with a certainty of 80%. Hence, we believe this 68-ps correlation time to be within ±20 ps of the correct value.

Additional anisotropy data are shown in Figure 6 for oxytocin and BPTI. In both cases, the differential phase angles show a bimodal distribution, which we attribute to motions and/or depolarization on substantially different time scales. The frequency range from 200 and 2000 MHz is important because it represents the transition from global rotational diffusion to segmental motions. Our previous results to 200 MHz indicated the shorter components in protein anisotropy decays, but these components were less evident in the data (Lakowicz et al., 1986a). For oxytocin, we recovered decay times of 29 and 454 ps. The values are probably due to tyrosyl motion and rotational diffusion of the oxytocin molecule, respectively. We again questioned the uncertainty in the shorter correlation time. Accordingly, the data were analyzed with this parameter held fixed at values ranging from 15 to 60 ps (Table III). Fixed values of 20 or 45 ps yield highly elevated values of χ_R^2 (2.5- or 6-fold, respectively), which indicates these values have probabilities of 10% or less. Evidently, the 2-GHz data provide narrow estimates of picosecond correlation times.

The anisotropy decay of BPTI also displays both rapid and slower components in the anisotropy decay (Table III). The 2–3-ns correlation time is approximately that expected for a

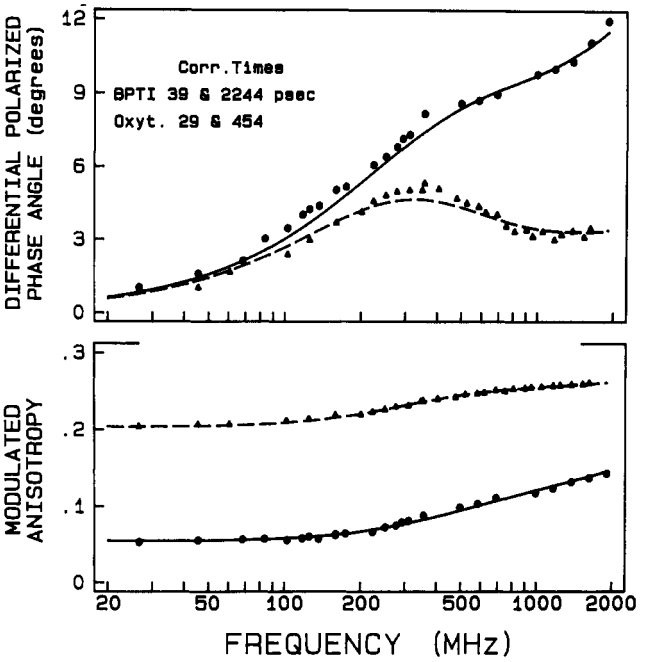

FIGURE 6: Differential phase and modulated data for oxytocin (●) and BPTI (▲) at 25 °C.

protein of this size (Lakowicz & Maliwal, 1983). BPTI contains four tyrosine residues, and steady-state measurements at low temperature indicated the likelihood of energy transfer among the tyrosyl residues (Lakowicz & Maliwal, 1983). Alternatively, a picosecond component in the anisotropy decay could be the result of the tyrosyl torsional motions predicted by molecular dynamics (Karplus & McCammon, 1981; van Gunsteren & Karplus, 1982; Karplus & McCammon, 1980). The data support the existence of a rapid but time-dependent depolarization process. This component is suggested by our inability to fit the data using a fundamental anisotropy of 0.27. This is the value we measured for BPTI in vitrified solution at −60 °C. These conditions should freeze out the motions, but energy transfer could still occur. Analysis using a variable value for r_0 resulted in an improved fit (2-fold decrease in χ_R^2) and an apparent r_0 value nearly equivalent to that of tyrosine itself (0.30 vs. 0.32). If the depolarization were instantaneous on our measurable time scale, the lower r_0 value of 0.27 would provide an adequate fit. We also note that the amplitude of the rapid component is comparable to that expected from the molecular dynamics calculations. These calculations predict torsional motions of the tyrosine residues of about 20° in a few picoseconds. It is not possible to select a precise value for the angular displacement because the amplitude of the events ranges from 7° to 30°. With an average value of 20°, the fractional anisotropy (r/r_0) remaining after these motions can be obtained from

$$\frac{r}{r_0} = \frac{3\cos^2\theta - 1}{2} \tag{15}$$

where θ is the angle through which the group is free to rotate. For $\theta = 30°$, the remaining anisotropy is 0.83. Hence, about 17% of the total anisotropy, or an amplitude of about 0.05, is expected to decay via a picosecond process. A similar conclusion is reached if one uses the "wobbling in a cone" model (Kinosita et al., 1977). Then

$$\frac{r}{r_0} = [(1/2)\cos\theta_m(1 + \cos\theta_m)]^2 \tag{16}$$

where the residue is assumed to randomize within a maximum

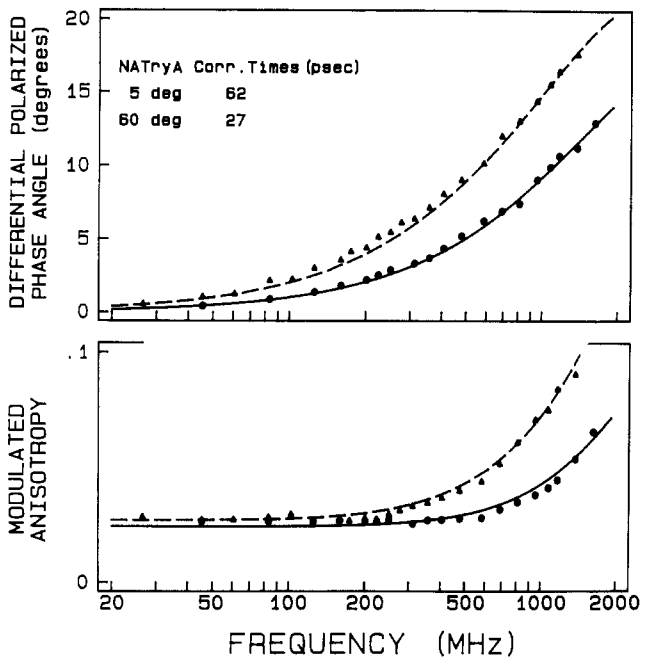

FIGURE 7: Picosecond anisotropy decays of *N*-acetyl-L-tyrosinamide in water. This sample contained 0.25 M KI to decrease the tyrosine decay time. The intensity decay parameters are in Table VI, and the anisotropy decay parameters are in Table IV. 5 °C (▲); 58 °C (●).

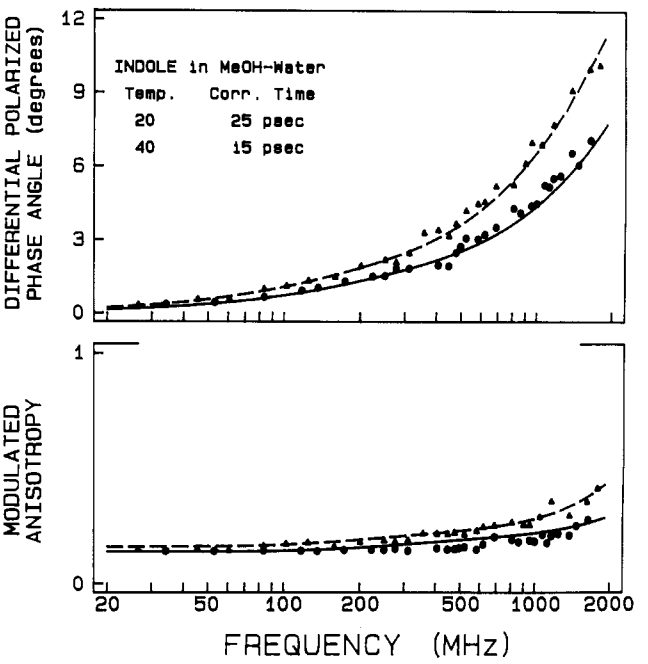

FIGURE 8: Picosecond anisotropy decays of indole in methanol/water (75/25). The sample contained 0.25 M KI to decrease the decay time. The decay parameters are in Table V. 20 °C (▲); 40 °C (●).

cone angle θ_m. For this model with $r_0 = 0.30$ and $\theta_m = 20°$, the amplitude of the rapid component in the anisotropy decay is near 0.05. These predicted values are also in agreement with the results of Kasprzak and Weber (1982), who used steady-state measurements of BPTI to determine that about 22% of the total anisotropy, or an amplitude of about 0.07, was lost by rapid processes not linked to overall rotational diffusion. Hence, the amplitude of the rapid component we detected agrees both with earlier steady-state data and with the prediction of molecular dynamics. However, the time scale of the process appears to be 10–100-fold longer than the molecular dynamics results. For instance, the fast anisotropy decay of BPTI was calculated to be complete in less than 2 ps (van Gunsteren & Karplus, 1982; Karplus et al., 1980; Levy & Szabo, 1982), whereas our measurements indicate a time scale of 39 ps. It should be noted that other molecular dynamics calculations on lysozyme indicated that the anisotropy of some tryptophan residues continued to decay after 15 ps (Ichiye & Karplus, 1983), so that our measured value of 35 ps is not unreasonable. Additionally, it was not possible to fit the data to a two-component anisotropy decay in which one of the decay times was fixed at 2 ps. This attempt resulted in a 6-fold increase in χ_R^2 and a small amplitude for the 2-ps component (Table III). The present data represent our first attempts on resolving the anisotropy decay of BPTI. Additional experimentation and analysis will be necessary to assign the 39-ps component in the anisotropy decay to either energy transfer or the torsional motions predicted from molecular dynamic calculations, and to further determine the time constant for the rapid component in the anisotropy decay.

Picosecond Anisotropy Decays. We questioned the lower limit of the correlation times we could determine. For this estimation, we examined NAcTyrA in aqueous solution from 5 to 58 °C (Figure 7 and Table IV). These solutions contained 0.25 M KI to decrease the tyrosine decay time and hence allow measurements to the 2-GHz limit. The intensity decay parameters are summarized in Table VI.

For NAcTyrA from 5 to 58 °C, the correlation times ranged from 62 to 27 ps (Table IV). The analyses were performed with both fixed and variable values of r_0. At 5 °C, the same anisotropy decay is obtained. For correlation times below 50 ps, it is important to use the known value of r_0 to stabilize the fit. Otherwise, the apparent values of r_0 are elevated above that expected for tyrosine.

Table V: Intensity Decay Parameters of NAcTyrA and Indole Solutions

sample	n^a	τ_i (ns)	$\alpha_i{}^b$	$f_i{}^c$	$\chi_R{}^{2\,d}$
indole, H_2O, 20 °C, no I^-	1	4.49	1.0	1.0	1.9
	2	3.50	0.16	0.12	
		4.67	0.84	0.88	1.6
indole, H_2O, 20 °C, 295 nm, 0.25 M KI	1	0.52	1.0	1.0	345
	2	0.30	0.75	0.45	
		1.10	0.25	0.55	4.3
indole, 75% MeOH, 0.25 M KI, 20 °C, 298 nm	1	0.41	1.0	1.0	539
	2	0.26	0.83	0.51	
		1.20	0.17	0.48	1.8
40 °C	1	0.30	1.0	1.0	632
	2	0.18	0.82	0.48	
		0.86	0.18	0.52	3.5
NAcTyrA + 0.25 M KI, 5 °C	1	0.70	1.0	1.0	139
	2	0.19	0.30	0.09	
		0.83	0.70	0.91	2.1
20 °C	1	0.61	1.0	1.0	73
	2	0.16	0.24	0.06	
		0.69	0.76	0.94	3.0
58 °C	1	0.37	1.0	1.0	221
	2	0.05	0.42	0.08	
		0.45	0.58	0.92	1.9

[a] Number of exponential components. [b] $\sum\alpha_i = 1.0$. [c] $\sum f_i = 1.0, f_i = \alpha_i\tau_i/\sum\alpha_i\tau_i$. [d] Calculated by using 0.2° and 0.005 as the standard deviations of the phase and modulation, respectively.

Surprisingly, even at 58 °C the phase angles at 2 GHz for NAcTyrA were well above our random error of 0.2–0.5°. Hence, we examined indole in water and methanol/water (75/25) (Figure 8). We suspected shorter correlation times because indole lacks the aminocarboxyl side chain of NAcTyrA. Once again, the mean decay time was decreased by iodide quenching. The intensity decay parameters are summarized in Table V. In the presence of quenching, the intensity decays became significantly multi- or nonexponential. We believe this is to be the result of the time-dependent terms

Table VI: Anisotropy Decays of Indole in Water and Methanol/Water (75/25)[a]

solvent	temp (°C)	θ (ps)	r_0	χ_R^2
water	20	53	⟨0.256⟩[b,c]	2.6
		51	0.263	2.7
		53	⟨0.256⟩[d]	2.8
		53		
MeOH/H_2O, 75/25	20	25	⟨0.290⟩[e]	1.7
		24	0.303	1.7
		24	0.156[d]	
		26	0.134	1.8
	40	15	⟨0.290⟩	2.6
		4	1.14	1.6
	40	23	⟨0.20⟩[f]	4.3
		18	⟨0.25⟩	3.1
		13	⟨0.35⟩	2.2
		11	⟨0.40⟩	2.0

[a] The solutions contained 0.25 M KI to decrease the decay time. The total concentration of KCl + KI was 0.25 M. The buffer (in 100% H_2O) was 0.05 M Tris, pH 7.0, containing a trace amount of $Na_2S_2O_3$. [b] The broken brackets indicate the r_0 value was held at this constant analysis in the analysis. The r_0 values were measured at −60 °C in propylene glycol. The lack of brackets indicates that the r_0 value was variable in the analysis. The underlined values indicates the fit we believe to be most appropriate. [c] 295-nm excitation. [d] The two correlation times are for fitting the data to two correlation times. [e] 298-nm excitation. [f] The fixed value of r_0 was varied to determine the effect of r_0 on the correlation time. See text for additional discussion.

in the diffusion equations which yield a $t^{1/2}$ dependence in the decay law (Ware & Nemzek, 1973; Nemzek & Ware, 1975). This phenomenon does not affect the present anisotropy analysis and will be the subject of a separate publication. In water at 20 °C, the correlation time was 53 ps (Table VI). At 25 °C in methanol/water, the correlation time was 25 ps. The uncertainty in this value from the usual assumptions of nonlinear least squares (Bevington, 1969) is 1 ps or less. We questioned the effect of an error in r_0 on this short correlation time and thus analyzed the data with various different but fixed values of r_0 (Table VI). The fit with $r_0 = 0.4$ yields a lower value of χ_R^2, but this value of r_0 is clearly too large for indole at 298-nm excitation. An r_0 value of 0.2 is clearly too low for indole, and in any event, this value results in a elevated value of χ_R^2. A range of r_0 values from 0.25 to 0.35 is certainly adequate to bracket the experimental uncertainty in our experimental value of 0.29. These r_0 values result in apparent correlation times of 14–20 ps. Hence, we believe our 15-ps correlation time to be accurate to ±3 ps or less. This importance of using the value of r_0, if known, is illustrated by the parameters obtained with r_0 as floating parameters. The apparent value of r_0 is obviously unacceptable. Examination of the data (Figure 8) shows a maximum phase angle of 7° at 2 GHz, which suggests that still shorter correlation times could be measured.

Indole is a flattened platelike molecule, and one expects its anisotropy decay to be multiexponential. In fact, we have recovered two correlation times for indole in the more viscous solvent propylene glycol (J. R. Lakowicz et al., unpublished observation). However, for the picosecond correlation times in Table VI it was not possible to recover more than a single correlation time. This is evident from the attempts to fit the data using two correlation times (Table VI). In each case, the two correlation times are equivalent, and the value of χ_R^2 was not decreased by the additional floating parameter.

Discussion

We previously used oxygen-quenching and steady-state anisotropy measurements (Maliwal & Lakowicz, 1983) to estimate the correlation times of the molecules described in this study. It is interesting to note that these very different methods yielded similar values for the overall correlation times and for the amplitudes of the picosecond depolarizing events. However, the quenching studies did not reveal the correlation times of the faster processes. The quenching method yielded global correlation times at 25 °C of 37, 100, 180, and 2706 ps for NAcTyrA, enkephalin, oxytocin, and BPTI, respectively. As observed by the quenching method, a fast component in the anisotropy decay was expected to yield smaller values for the apparent correlation time, this explaining the shorter correlation for enkephalin and oxytocin obtained from the quenching studies. Additionally, the quenching studies indicated that the total anisotropy of BPTI was not accounted for by the 2.9-ns component, and the amplitude of the missing anisotropy is comparable to the present higher resolution measurements on this same molecule.

The results in Figures 1–3 and Table II illustrate several features of the frequency-domain method. First, it provides remarkable resolution of the complex decay laws on the subnanosecond time scale. One reason is thta the 4–2000-MHz frequency range is ideally suited for this time scale. Second, the degree of random error in the data is small, which allows complex decays or multiple parameters to be recovered from the data. We stress that the good fits provided by the two or three decay time models do not prove that the decay law is actually a double or triple exponential. Rather, the goodness of fit only indicates these models are adequate. We are presently analyzing these and other similar data with decay time distributions.

The data for NAcTyrA in Figure 2 illustrate another important feature of the gigahertz frequency-domain data. For NAcTyrA, the frequency range of the measurements was limited by the relatively long lifetime of NAcTyrA (1.5 ns), rather than by the bandwidth of the instrument. This is because at high modulation frequencies the 1.5-ns decay time results in an 80% loss of the modulated emission of 500 MHz. Consequently, the degree of random error in the phase angles increases. This intrinsic demodulation is less of a problem with the tyrosyl peptides and proteins because the decay times are somewhat smaller and the fractional amplitude of the short-lived component is greater, resulting in higher modulation at frequencies above 500 MHz (Figures 2 and 3). For NAcTyrA and indole, we circumvented the intrinsic demodulation problem by decreasing the decay time using iodide quenching.

We believe that gigahertz frequency-domain fluorometry will be especially useful for the resolution of complex anisotropy decays on the subnanosecond time scale. This is illustrated by the highly variable differential phase angle profiles observed for the various peptides (Figures 5 and 6). Such detailed information should allow a comparison of experimentally determined anisotropy decays with decays predicted by various hydrodynamic models, including segmental motions of portions of the rotating molecule.

Finally, we note that the 2-GHz frequency-domain data will allow measurements of correlation times as short as 15 ps. Hence, the experimental time resolution of the frequency-domain measurements now overlaps with the time scale of molecular dynamics calculations. A comparison of experimental data with theory is now possible.

Acknowledgments

J.R.L. especially thanks Dr. Shinoda and the Hamamatsu Co. for donating the microchannel plate PMT and Fred Gonzalez (Coherent, Inc.) for his assistance in installing the picosecond laser system. J.R.L. explicitly thanks the National Science Foundation for supporting development of the fre-

quency-domain method at a time when others thought the instrumentation could not be developed.

Registry No. BPTI, 9035-81-8; Enk, 58822-25-6; NAcTyrA, 1948-71-6; L-Tyr, 60-18-4; PhOH, 108-95-2; oxytocin, 50-56-6; rose bengal, 11121-48-5; indole, 120-72-9.

REFERENCES

Albani, J., Alpert, B., Krajcarski, D. T., & Szabo, A. G. (1985) *FEBS Lett. 182*, 302–304.

Bevington, P. R. (1969) *Data Reduction and Error Analysis for the Physical Sciences*, McGraw-Hill, New York.

Brand, L., Knutson, J. R., Davenport, L., Beechem, J. M., Dale, R. E., Walbridge, D. G., & Kowalczyk, A. A. (1985) in *Spectroscopy and the Dynamics of Molecular Biological Systems* (Bayley, P. M., & Dale, R. E., Eds.) Academic Press, New York.

Cundall, R. B., & Dale, R. E. (1980) *Time-Resolved Fluorescence Spectroscopy in Biochemistry and Biology*, Plenum Press, New York.

Gauduchon, P., & Wahl, Ph. (1978) *Biophys. Chem. 8*, 87–104.

Gratton, E., & Lopez-Delgado, R. (1980) *Nuovo Cimento Soc. Ital. Fis., B 56B*, 110–124.

Gratton, E., & Limkeman, M. (1983) *Biophys. J. 44*, 315–324.

Gratton, E., Jameson, D. M., Rosato, N., & Weber, G. (1984) *Rev. Sci. Instrum. 55*, 486–494.

Ichiye, T., & Karplus, M. (1983) *Biochemistry 22*, 2884–2893.

Karplus, M., & McCammon, J. A. (1981) *CRC Crit. Rev. Biochem. 9*, 293–349.

Karplus, M., Gelin, B. R., & McCammon, J. A. (1980) *Biophys. J. 32*, 603–618.

Kinosita, K., Kawato, S., Ikegami, A. (1977) *Biophys. J. 20*, 289–305.

Lakowicz, J. R. (1985) *Spectroscopy 1*, 28–32.

Lakowicz, J. R. (1986) *Methods Enzymol. 131*, 518–567.

Lakowicz, J. R., & Maliwal, B. P. (1983) *J. Biol. Chem. 258*, 4794–4801.

Lakowicz, J. R., & Maliwal, B. P. (1985) *Biophys. Chem. 21*, 61–78.

Lakowicz, J. R., Gratton, E., Laczko, G., Cherek, H., & Linkemann, M. (1984a) *Biophys. J. 46*, 463–477.

Lakowicz, J. R., Gratton, E., Cherek, H., Maliwal, B. P., & Laczko, G. (1984b) *J. Biol. Chem. 259*, 10967–10972.

Lakowicz, J. R., Cherek, H., Maliwal, B., & Gratton, E. (1985) *Biochemistry 24*, 376–383.

Lakowicz, J. R., Laczko, G., Gryczynski, I., & Cherek, H. (1986a) *J. Biol. Chem. 261*, 2240–2245.

Lakowicz, J. R., Laczko, G., & Gryczynski, I. (1986b) *Rev. Sci. Instrum. 57*, 2499–2506.

Laws, W. R., Ross, J. B. A., Wyrsbrod, H. R., Beechem, J. M., Brand, L., & Sutherland, J. C. (1986) *Biochemistry 25*, 599–607.

Lee, J., O'Kane, D. J., & Visser, A. S. W. G. (1985) *Biochemistry 24*, 1476–1483.

Levy, R. M., & Szabo, A. (1982) *J. Am. Chem. Soc. 104*, 2073–2075.

Libertini, L. J., & Small, E. W. (1985) *Biophys. J. 47*, 765–772.

Ludescher, R. D., Volwerk, J. J., de Haas, G. H., & Hudson, B. S. (1985) *Biochemistry 24*, 7240–7249.

Maliwal, B. P., & Lakowicz, J. R. (1986) *Biochim. Biophys. Acta 873*, 161–172.

Nemzek, T. C., & Ware, W. R. (1975) *J. Chem. Phys. 62*, 477–489.

O'Connor, D. V., & Phillips, D. (1985) *Time-Correlated Single Photon Counting*, Academic Press, New York.

van Gunsteren, W. F., & Karplus, M. (1982) *Biochemistry 21*, 2259–2274.

Ware, W. R., & Nemzek, T. L. (1973) *Chem. Phys. Lett. 23*, 557–560.

Wilson, J., & Hawkes, J. F. B. (1983) *Optoelectronics: An Introduction*, p 431, Prentice-Hall, Englewood Cliffs, NJ.

Yamazaki, I., Tamai, N., Kume, H., Tsuchiya, H., & Oba, K. (1985) *Rev. Sci. Instrum. 56*, 1187–1194.